




Review

An Insight into All Tested Small Molecules against *Fusarium oxysporum* f. sp. *Albedinis*: A Comparative Review

Yassine Kaddouri ¹, Redouane Benabbes ², Sabir Ouahhoud ², Magda Abdellattif ^{3,*} , Belkheir Hammouti ⁴ 
and Rachid Touzani ^{4,*} 

- ¹ Laboratory of Inorganic Chemistry, Department of Chemistry, University of Helsinki, P.O. Box 55, FI-00014 Helsinki, Finland; y.kaddouri@ump.ac.ma
- ² Laboratoire de Bioressources, Biotechnologie, Ethnopharmacologie et Santé (LBBES), Department of Biology, Faculty of Sciences, University Mohamed Premier, Oujda 11022, Morocco; red.bes72@gmail.com (R.B.); ouhaddouch@yahoo.fr (S.O.)
- ³ Chemistry Department, College of Sciences, Taif University, P.O. Box 11099, Taif 21944, Saudi Arabia
- ⁴ Laboratory of Applied Chemistry and Environment (LCAE), Faculty of Sciences, University Mohammed Premier, Oujda 11022, Morocco; hammoutib@gmail.com
- * Correspondence: m.hasan@tu.edu.sa (M.A.); r.touzani@ump.ac.ma (R.T.)

Abstract: Bayoud disease affects date palms in North Africa and the Middle East, and many researchers have used various methods to fight it. One of those methods is the chemical use of synthetic compounds, which raises questions centred around the compounds and common features used to prepare targeted molecules. In this review, 100 compounds of tested small molecules, collected from 2002 to 2022 in Web of Sciences, were divided into ten different classes against the main cause of Bayoud disease pathogen *Fusarium oxysporum* f. sp. *albedinis* (F.o.a.) with structure–activity relationship (SAR) interpretations for pharmacophore site predictions as ($\delta^- \dots \delta^-$), where 12 compounds are the most efficient (one compound from each group). The compounds, i.e., (Z)-1-(1,5-Dimethyl-1H-pyrazole-3-yl)-3-hydroxy but-2-en-1-one **7**, (Z)-3-(phenyl)-1-(1,5-dimethyl-1H-pyrazole-3-yl)-3-hydroxyprop-2-en-1-one **23**, (Z)-1-(1,5-Dimethyl-1H-pyrazole-3-yl)-3-hydroxy-3-(pyridine-2-yl)prop-2-en-1-one **29**, and 2,3-bis-[(2-hydroxy-2-phenyl)ethenyl]-6-nitro-quinoxaline **61**, have antifungal pharmacophore sites ($\delta^- \dots \delta^-$) in common in N1–O4, whereas other compounds have only one δ^- pharmacophore site pushed by the donor effect of the substituents on the phenyl rings. This specificity interferes in the biological activity against F.o.a. Further understanding of mechanistic drug–target interactions on this subject is currently underway.

Keywords: pyrazole; imidazole; B-keto-enol; amino acid; quinoxaline; Bayoud; *Fusarium oxysporum* f. sp. *albedinis*



Citation: Kaddouri, Y.; Benabbes, R.; Ouahhoud, S.; Abdellattif, M.; Hammouti, B.; Touzani, R. An Insight into All Tested Small Molecules against *Fusarium oxysporum* f. sp. *Albedinis*: A Comparative Review. *Molecules* **2022**, *27*, 2698. <https://doi.org/10.3390/molecules27092698>

Academic Editor: Jussara Amato

Received: 6 February 2022

Accepted: 18 April 2022

Published: 22 April 2022

Publisher's Note: MDPI stays neutral with regard to jurisdictional claims in published maps and institutional affiliations.



Copyright: © 2022 by the authors. Licensee MDPI, Basel, Switzerland. This article is an open access article distributed under the terms and conditions of the Creative Commons Attribution (CC BY) license (<https://creativecommons.org/licenses/by/4.0/>).

1. Introduction

Bayoud disease [1–5], caused by the telluric fungus pathogen *Fusarium oxysporum* f. sp. *albedinis* (F.o.a) [6–9], represents the leading dangerous agent of date palms cultivation, having killed more than 15 million Moroccan and Algerian date palm trees. Fungal infection causes significant implications, threatening date palms with high morbidity and mortality every year worldwide. Therefore, new antifungal inhibitors must be discovered urgently, especially those with new modes of action, low toxicity, and bioavailability, and are effective for responsive and drug-resistant fungi [10–15]. Due to their biological activity and chemical properties in recent years, fused heterocyclic compounds containing bridgehead nitrogen or oxygen donor atoms have drawn further interest. Indeed, several classes are reported in this review as pyrazole- and imidazole-based derivatives [16] presented in different biomolecules, such as histidine [17], histamine [18], and natural products [19]; this is an exciting building block [20]. Specifically, in recent decades, 4,5-diarylpyrazoles [21] and 2,5-diarylimidazoles [22] have gained interesting recognition as possible biomolecules in

the field of drug development. Many biological and pharmacological properties are related to these structures [23]. β Keto-enol compounds [24–27] are found in many natural products as coumarin derivatives and play an important role in medicine and in the development of coordination chemistry as stable complexes. Imidazothiazole derivatives [28–30] are attractive nitrogen-containing heterocyclic ring-like histidine, biotin, nucleic acid, purine, etc., and have a broad spectrum of biological and pharmacological diverse activities.

Pyrazolic compounds [31] have established widespread potential biological activities, such as anti-inflammatory [32–34], antianxiety [35], antipyretic [36], antimicrobial [37–40], antiviral [41], antitumor [42–44], anticonvulsant [36,45–47], etc. Quinoxalines [48] are polyfunctionalized compounds with interesting biological activities, such as anti-human immunodeficiency virus (anti-HIV) and antidiabetic agents. Benzimidazole-1,2,3-triazole hybrid molecules [49] are hybrid compounds consisting of benzimidazole and 1,2,3-triazole, where both of them have a broad range of biological activities. *N,N'*-bipyrazole piperazine derivatives [50] are established as polypharmacological mixed ligands with several biological activities reported in the literature [51–54]. Meanwhile, Schiff base derivatives [53] have different biological functions, such as anti-inflammatory [55], antifungal [56], and antibacterial effects [57], and are commonly used as carriers of catalysts [58], optical chemical receptors [59], thermo-stable products [60], agents of metal complexation [61], inhibitors of corrosion [62], and stabilizers of polymers [63].

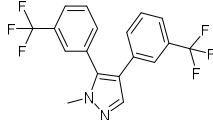
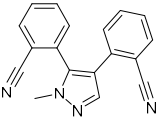
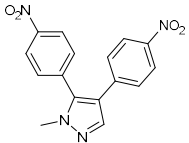
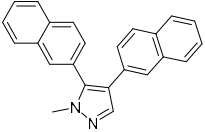
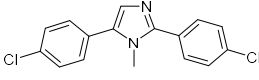
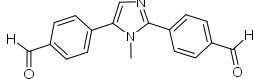
2. Pyrazole- and Imidazole-Based Derivatives

After some modifications, the agar diffusion approach is used for the antifungal analysis of pyrazole- and imidazole-based derivatives. In short, after isolation and preparation of the *Fusarium* fungus, the sterilized solution of the six compounds tested (1–6) in dimethyl sulfoxide (DMSO) is mixed with the potato dextrose agar (PDA) medium as an emulsifier at different concentrations using the method mentioned in the literature [16]. These compounds were synthesized by Takfaoui et al. using direct arylation of pyrazoles and imidazoles with aryl halides, using palladium as the catalyst, DMAc as the solvent, and CsOAc as the base [64,65].

Using a non-linear regression algorithm curve of the concentration/percentage of inhibition, the half-maximal inhibitory concentration (IC_{50}) was measured using Graphpad Prism software. DMSO-distilled water mixture was used as the negative control; no recognized antibiotic can specifically treat this infection.

The IC_{50} values are given in (Table 1) below. In the pyrazole derivatives, compound 4 ($IC_{50} = 99.1 \mu\text{g/mL}$) has the best fungus inhibition of all the tested compounds, where it contains *p*- C_6H_4 groups on the phenyl rings as an electron-donating character, and the high toxicity effect of the phenyl groups on the F.o.a. Furthermore, compound 1 ($IC_{50} = 110.9 \mu\text{g/mL}$), presenting *m*- CF_3 groups on both phenyl rings, displays good activity close to that of compound 4. However, the following compound is from the imidazole series (compound 5) containing *p*-Cl groups on phenyl rings with an IC_{50} value equal to $114.7 \mu\text{g/mL}$. The substitution of the phenyl rings by formyl (COH) groups (compound 6) is highly unfavorable for inhibitory potency [16].

Table 1. IC₅₀ values of the tested pyrazole- and imidazole-based derivatives tested against F.o.a.

ID.	Structure	IC ₅₀	
		µg/mL	µM
1		110.9	299.4
2		153.2	538.8
3		165.1	509.1
4		99.1	256.4
5		114.7	378.3
6		194.5	667.1

Compared with literary works, we found that the pyrazole skeleton and its derivatives exhibited excellent inhibitory activity against *Fusarium oxysporum* [66].

3. β-Keto-enol Derivatives

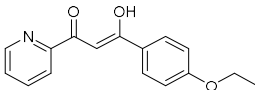
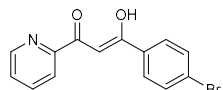
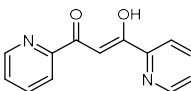
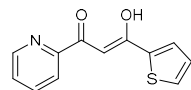
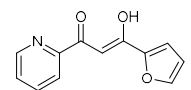
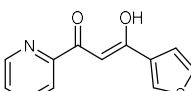
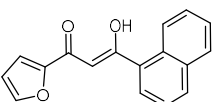
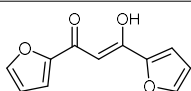
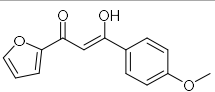
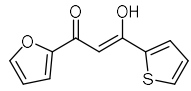
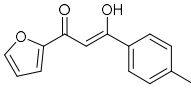
a β-Keto-enol Pyridine and Furan Derivatives

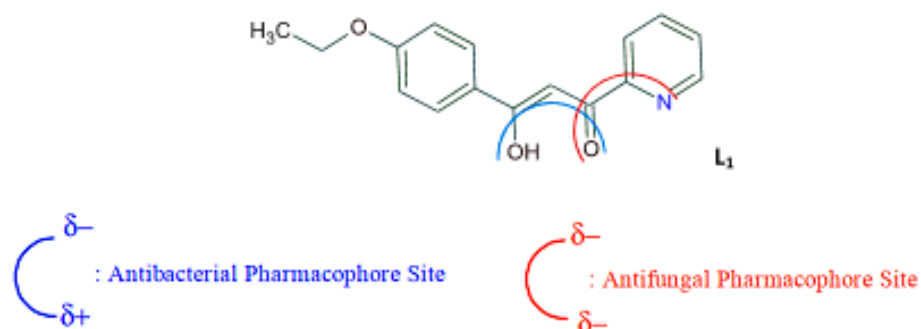
Using the agar diffusion process, we determined the in vitro antifungal ability of 11 compounds (7–17) against the pathogenic fungus (F.o.a). The synthetic route of the target compounds (7–17) was carried out following Claisen condensation under mild conditions [24,26,67–74]. Using the protocol described in the literature [27], the percentages of inhibition and semi-maximal inhibitory concentration (IC₅₀) were measured and estimated using the inhibition percentage non-linear regression equation, while benomyl was used as a positive control (Table 2).

As presented in Table 2, the fungal activity of 7 is very substantial, though it decreases slightly in the case of 10 because of ethoxy phenyl groups, which commonly have pharmacophore sites ($\delta^- \cdots \delta^+$), as presented in Figure 1, due to their physicochemical properties and their ability to penetrate the envelope of fungal cells and enter their cellular place of action, thus displaying more excellent activity in [27].

b (Z)-3(3-bromophenyl)-1-(1,5-dimethyl-1H-pyrazol-3yl)-3-hydroxyprop-2-en-1-one derivatives

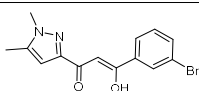
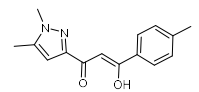
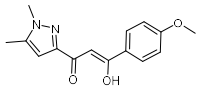
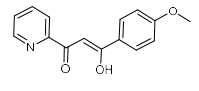
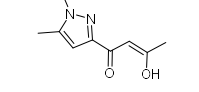
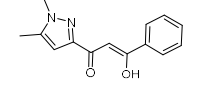
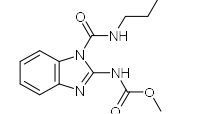
Table 2. IC₅₀ values of the tested β keto-enol pyridine and furan derivatives against F.o.a.

ID	Structure	IC ₅₀	
		$\mu\text{g/mL}$	μM
7		12.83	
8		NS	NS
9		NS	NS
10		17	
11		36	
12		-	-
13		-	-
14		-	-
15		-	-
16		-	-
17		-	-

**Figure 1.** Antibacterial and antifungal pharmacophore sites for compound 7.

The agar diffusion technique was tested for in vitro antifungal function (ADT), where the literature reported the protocol details [7]. The optical density values were measured for each culture at 625 nm, and the inhibition percentage (%) is expressed as $(D_0 - D_x)/D_0 \times 100$. D_0 is the diameter of the mycelial growth of the culture witness, and D_x is the diameter of the mycelial growth (Table 3). The target biomolecules 18–23 based on β keto-enol and pyrazole entities and pyridine were prepared using a one-pot in situ condensation method, similar to the procedures in the literature [24].

Table 3. Volume is withdrawn, a diameter of the strain and inhibition percentages of the tested (Z)-3(3-bromophenyl)-1-(1,5-dimethyl-1H-pyrazole-3-yl)-3-hydroxyprop-2-en-1-one derivatives 18–23 against F.o.a.

ID	Structure	Volume Is Withdrawn (μ L)	Diameter of the Strain in the Presence of the Drug (cm)	Inhibition (%)
18		50	5.0	0
		200	3.8	24
		500	2.7	46
19		50	5.0	0
		200	3.5	30
		500	2.3	54
20		50	5.0	0
		200	3.6	28
		500	2.5	50
21		50	5.0	0
		200	3.8	24
		500	3.2	36
22		50	1.2	76
		200	0.9	82
		500	0.5	90
23		50	2.0	60
		200	1.3	74
		500	0.2	96
Benomyl		50	2.3	54
		200	1.1	78
		500	0.3	94

As presented in Table 3, only compounds 22 and 23 reach values close to the standard (benomyl), as they belong to the same family. Such variations depend on the radical group attached to the fragment of pyrazole keto-enol, where compound 23 has a phenyl ring attached instead of the methyl group in compound 22. In addition, numerous molecular improvements are currently being made to these compounds as antifungal candidates [25].

c β -Keto-enol pyrazolic compounds

The in vitro antifungal potential of ten prepared β Keto-enol pyrazolic compounds against the pathogen F.o.a was determined by the agar diffusion technique reported in the literature [26], and the half-maximal inhibitory concentration (IC_{50}) was determined using a non-linear regression algorithm of the concentration-inhibition percentage graph, with benomyl used as a positive control. In addition, the target biomolecules 24–30 based on β keto-enol and pyrazole entities were prepared by a one-pot in situ condensation method, which is similar to the procedures given in the literature [24].

On the other hand, most of these molecules demonstrate potent antifungal action against F.o.a, as seen in Table 4. These were based on the structure–activity relationships

(S.A.R.s). Where a stimulating effect is exerted against F.o.a of the substitution pattern, we found compound **28** in the 3-thiophene group. In contrast, compound **30** with the 2-naphthalene group led the same inhibition percentage of 94% as the benomyl fungicide, while the best antifungal activity was found for compound **29** containing the 2-pyridine group IC₅₀ of 60.84 µg/m. The existence of the R substituent should be further exploited [8] to evaluate the S.A.R.s for this novel class of antifungal agents.

Table 4. IC₅₀ values of the tested βketo-enol pyrazolic derivatives against F.o.a.

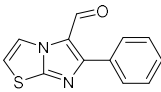
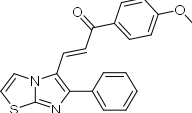
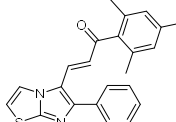
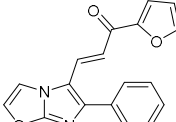
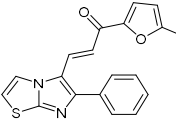
ID	Structure	IC ₅₀	
		µg/mL	µM
24		-	-
25		260.74	71
26		-	-
27		-	-
28		193.31	48.00
29		60.84	14.80
30		181.30	53.00

4. Imidazothiazole Derivatives

The synthesis of various types of imidazothiazoles **31–35** is potentially helpful for developing biologically active heterocycles. The synthetic methods are practical and straightforward and are conceivably applicable to analogous heterocyclic systems possessing nitrogen and sulfur [30,75–82]. The antifungal action of five imidazothiazole derivatives **31–35** is carried out on an F.o.a using the concentrations C₁, C₂, C₃, C₄, and C₅ as 5.0, 1.0, 0.2, 0.05, and 0.01 mg/mL, respectively. Each compound was prepared at various concentrations in the potato dextrose agar (PDA) before the fungus was cultured using the protocol described in the literature [28]. The IC₅₀ was calculated using the linear regression equation between the normal logarithm concentrations and growth inhibition percentages.

From Table 5, the antifungal test of the five imidazothiazole derivatives tested against F.o.a. at five different concentrations acted differently, while all the molecules showed interesting results. Indeed, the best antifungal activity is found for compound **33** due to three methyl substituents on the ortho and para positions of the phenyl ring with IC₅₀ not exceeding 20.00 µg/mL [28].

Table 5. IC₅₀ values of the tested imidazothiazole derivatives against F.o.a.

ID	Structure	IC ₅₀ (µg/mL)
31		50.00
32		70.00
33		20.00
34		60.00
35		50.00

5. Pyrazolic Compounds

Monopyrazolic heterocyclic compounds **36–55** were prepared in excellent yields by condensing one equivalent of hydroxymethylpyrazole with one equivalent of primary amines [83–85]. The antifungal behavior, as defined in the literature, was calculated by the agar diffusion technique [31], with the linear regression equation between the normal logarithm of the concentrations and the growth inhibition percentages calculated at the half-maximal inhibitory concentration (IC₅₀).

The pyrazolic derivatives **50**, **51**, and **53–55** were screened in vitro for their antifungal potential against F.o.a and collected in Table 6, where compounds **50** and **55** showed an excellent efficacy of IC₅₀ = 86 µM and 168 µM, respectively, arguably due to the presence of the two phenyl moieties. Due to the (-Br) group, which is an essential source of electronegativity, compound **53** showed a moderate potential with an IC₅₀ = 284 µM. The two other pyrazoles tested demonstrated low antifungal function [31].

Table 6. IC₅₀ values of the tested pyrazolic compounds against F.o.a.

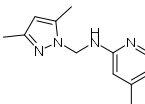
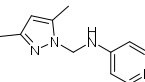
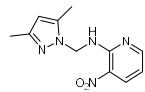
ID	Structure	IC ₅₀ (µM)
36		-
37		751
38		2507

Table 6. Cont.

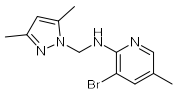
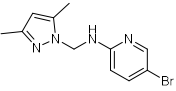
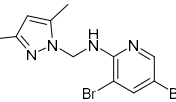
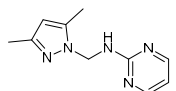
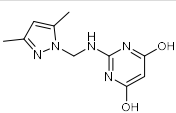
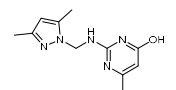
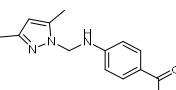
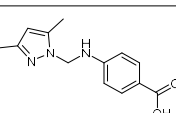
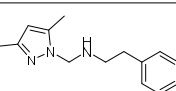
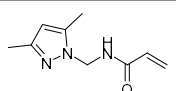
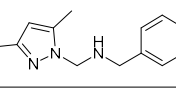
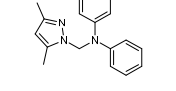
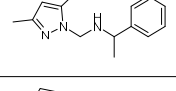
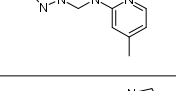
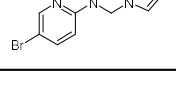
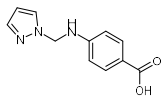
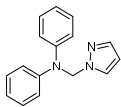
ID	Structure	IC ₅₀ (μM)
39		406
40		398
41		333
42		2755
43		2550
44		2486
45		2614
46		1223
47		697
48		2856
49		2322
50		86
51		662
52		2592
53		284

Table 6. Cont.

ID	Structure	IC ₅₀ (μM)
54		-
55		168

6. Quinoxalines

A variety of 2,3-bifunctionalized quinoxalines (**56–61**) have been prepared by the condensation of 1,6-disubstituted-hexan-1,3,4,6-tetraones with *o*-phenylenediamine, (*R,R*)-1,2-diaminocyclohexane, and *p*-nitro-*o*-phenylenediamine [86–88]. The antifungal activity of six prepared quinoxaline compounds' antifungal activity was measured against *F.o.a.*, as described in the method in the literature [48].

Based on Table 7, the most effective inhibitor is nitroquinoxaline **61**, which produces 51% inhibition of the growth of *Fusarium* at a concentration of 72 mg/L due to its small nitro groups that disturb the cell membrane, with some intracellular target and electron-withdrawing solid group. At the same time, compounds **56**, **60**, and **59** are less effective but produce appreciable growth inhibition at comparable concentrations [48].

Table 7. Percent growth inhibition at different concentrations for quinoxaline compounds tested against *F.o.a.*

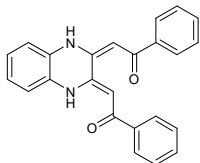
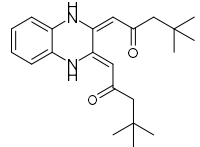
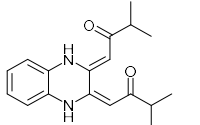
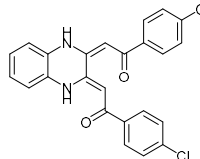
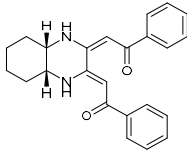
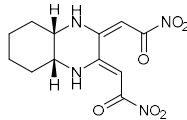
ID	Structure	Percent Growth Inhibition (Concentration, mg/L)		
		C1	C2	C3
56		9 (20)	7 (40)	22 (80)
57		9 (60)	15 (120)	15 (180)
58		17 (60)	17 (120)	19 (180)
59		21	32	35 (180)

Table 7. Cont.

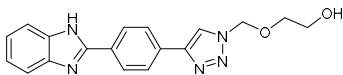
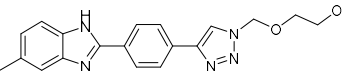
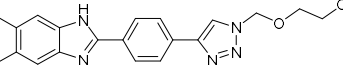
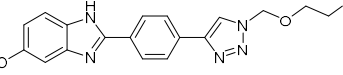
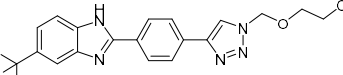
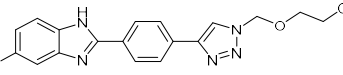
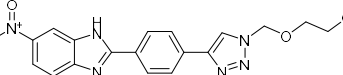
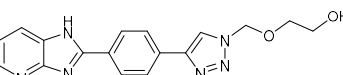
ID	Structure	Percent Growth Inhibition (Concentration, mg/L)		
		C1	C2	C3
60		15 (34)	31 (67)	33 (134)
61		29 (18)	31 (36)	51 (72)

7. Benzimidazole-1,2,3-triazole Hybrid Molecules

A series of hybrid molecules **62–69** was prepared by condensing 4- (trimethylsilylethynyl)benzaldehyde with substituted *o*-phenylenediamines. These, in turn, were reacted with 2-(azidomethoxy)ethyl acetate in a Cu alkyne–azide cycloaddition (CuAAC) to generate the 1,2,3-triazole pharmacophore under microwave assistance [89–92].

The eight new benzimidazole-1,2,3-triazole hybrid molecules were tested against *F.o.a* using the method described in the literature [49], and their linear growth and sporulation inhibitory rates are presented in Table 8.

Table 8. Linear growth and inhibitory sporulation rates of benzimidazole-1,2,3-triazole hybrid molecules tested against *F.o.a*.

ID	Structure	Linear Growth-Inhibitory Rates (%)	Sporulation Inhibitory Rates (%)
62		3.02 ± 0.96	−5.85 ± 0.04
63		−1.59 ± 0.05	16.36 ± 0.2
64		2.7 ± 0.16	−34.79 ± 0.72
65		−0.16 ± 0.02	21.94 ± 0.26
66		17.01 ± 0.96	30.62 ± 0.5
67		2.3 ± 0.29	−77.59 ± 2.64
68		−1.41 ± 0.3	−61.05 ± 1.34
69		−14 ± 0.05	−48.72 ± 2.35

Based on Table 8, all compounds were tested at a 20 mg/mL concentration, with Pelt, a systemic fungicide and benzimidazole precursor (70% of methyl thiophanate), as the positive control. Compound 66 shows a significantly increased rate with (17.01 and 30.62%) ($p < 0.05$) against F.o.a, which uniquely holds a CF_3 group fixed to the benzimidazole core, a lipophilic group known to modulate absorption and metabolism, and may explain the enhanced activity [49].

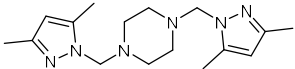
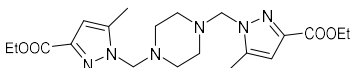
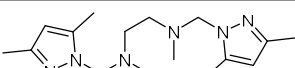
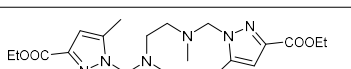
8. *N,N'*-Bipyrazole Piperazine Derivatives

Novel bipyrazoles 70–73 possessing piperazine or a mimed piperazine ring spacer were prepared in a one-step reaction in excellent yields. First, it condensed two hydroxymethylpyrazole derivatives with one equivalent of cyclic and acyclic piperazine [93–96].

As stated in the literature, in vitro antibacterial and antifungal activity is tested by the agar diffusion technique [50] using pathogenic strains of F.o.a. In contrast, streptomycin was used in the antibacterial assay as a reference compound for quality reasons. Therefore, the minimal concentration of inhibition (M.I.C.) is the lowest concentration of the tested compound that has inhibited the development of the micro-organism.

As presented in Table 9, four tested compounds showed differential anti-proliferative activity against F.o.a, as the best M.I.C. value was found for compound 71 of 5 $\mu\text{g/mL}$. These results are explained by the piperazine ring spacer and the carboxylate moiety at the three-position of the pyrazole rings that considerably increases the antifungal activity [50].

Table 9. M.I.C. values of *N,N'*-bipyrazole piperazine derivatives tested against F.o.a.

ID	Structure	M.I.C.	
		$\mu\text{g/mL}$	μM
70		10	33.06
71		5	11.94
72		10	32.85
73		20	47.56

9. Bipyrazolic Tripodal Derivatives

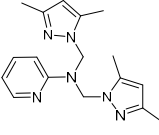
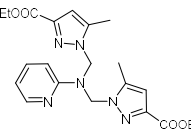
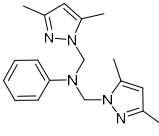
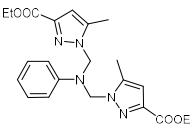
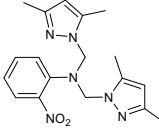
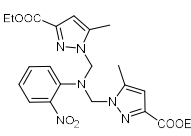
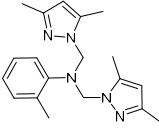
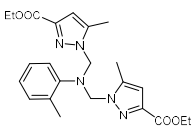
A series of novel bipyrazolic tripodal derivatives 74–81 was prepared in one step, with good and excellent yields. Then, one equivalent of the appropriate amine derivatives was added to a solution of two equivalents of the substituted hydroxymethylpyrazole in acetonitrile, and the mixture was continued under stirring at room temperature for 4–5 days. Finally, the crude material was evaporated, washed with water and CH_2Cl_2 , and purified by silica gel column flash chromatography to give the target product 74–81 [52].

The eight compounds containing bipyrazolic tripod derivatives are tested in vitro for their efficacy against *Fusarium oxysporum* f. Isolated from a date palm with vascular fusariosis, F.o.a was used as the protocol described in the literature [52]. The minimum inhibition concentration (M.I.C.) is the lowest dose of the compound that can inhibit micro-organism development.

From data in Table 10, the presence of the methyl as electron donor groups on the pyrazole rings increased the antifungal activity for compounds 74, 76, 78, and 80, but has a counter effect on the phenyl ring, e.g., in the case of compounds 80 and 81 which have M.I.C. values of 40 and 80 $\mu\text{g/mL}$, respectively. Additionally, nitro substituent

as an electron-withdrawing group for compound **79** increased its effect compared with compound **77** [52].

Table 10. M.I.C. values of bipyrazolic tripodal compounds tested against F.o.a.

ID	Structure	M.I.C.	
		$\mu\text{g/mL}$	μM
74		2.5	8.05
75		5	11.73
76		2.5	8.08
77		40	94.7
78		2.5	7.05
79		5	10.63
80		40	123.84
81		80	182.14

10. Schiff Base Derivatives

Twelve new Schiff base derivatives are prepared using the condensation reaction of different amino-substituted compounds (such as aniline, pyridine-2-amine, o-toluidine, 2-nitrobenzamine, 4-aminophenol, and 3-aminopropanol) and substituted aldehydes (such as nicotinaldehyde, o,m,p-nitrobenzaldehyde, and picolinaldehyde) in ethanol with acetic acid as a catalyst [53].

The agar diffusion technique against *Fusarium oxysporum f* evaluated the in vitro anti-fungal activities of all the new Schiff base derivative compounds, including F.o.a fungus, as described earlier [53]. In the presence of a concentration of the tested compound over the mycelium diameter of the reference culture multiplied by 100, it is found that the inhibition

proportion of a molecule is proportional to the ratio of the mycelium diameter of the culture. Therefore, the minimal concentration of inhibition (M.I.C.) is the lowest dose of the compound, which inhibited the growth of the microorganism when the mixture (DMSO/EtOH + distilled water) is used as a negative control without any standard reference drug.

On the contrary, based on their M.I.C. values in Table 11, the in vitro antifungal assay findings showed that most of the screened ligands exhibited high to moderate activity against F.o.a. The maximum activity was 0.02 $\mu\text{g/mL}$, shown by compound 84, followed by compounds 87, 88, and 93 with M.I.C. values equal to 0.04 $\mu\text{g/mL}$, while compound 83 showed the most negligible M.I.C. value of 0.9 $\mu\text{g/mL}$. Other products also have numerous activities, with M.I.C.s varying from 0.08 $\mu\text{g/mL}$ for compound 92 to 0.30 $\mu\text{g/mL}$ for compound 86. Comparing both the structures of 83 and 84, it can be inferred that the presence at the ortho position of the phenyl ring of a strong electron-withdrawing group, such as nitro moiety (NO_2), is very appropriate for increasing antifungal efficiency; the presence of an electron donation group, such as methyl moiety (CH_3) for antifungal action, is unfavorable in the period. Unfortunately, though, the correct variables that influence the antifungal ability of these derivatives are difficult to ascertain with these early investigations. Further investigations using other models and techniques are essential for this [53].

Table 11. M.I.C. values of Schiff base derivatives compounds tested against F.o.a.

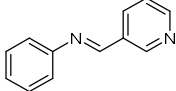
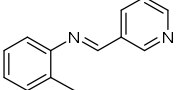
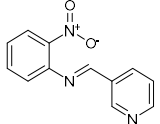
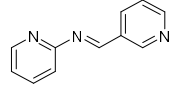
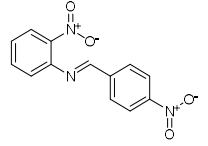
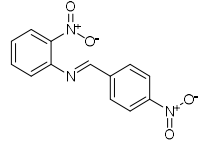
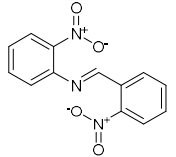
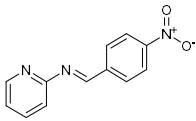
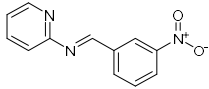
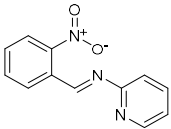
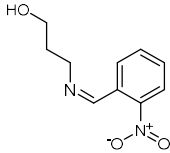
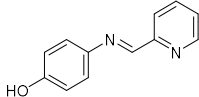
ID	Structure	MIC ($\mu\text{g/mL}$)
82		0.10
83		0.90
84		0.02
85		0.25
86		0.30
87		0.04
88		0.04

Table 11. Cont.

ID	Structure	MIC ($\mu\text{g/mL}$)
89		0.12
90		0.25
91		0.20
92		0.08
93		0.04

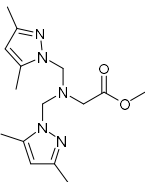
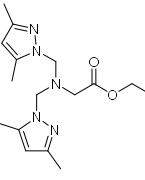
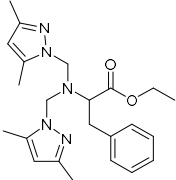
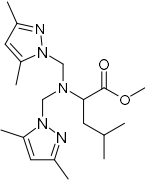
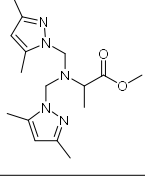
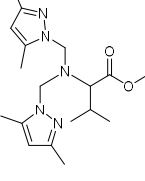
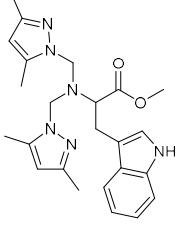
11. Amino Acids Pyrazole Compounds

The functional pyrazolyl derivatives **94–100** were prepared by condensing two equivalents of (3,5-dimethyl-1H-pyrazole-1-yl)methanol with one equivalent of amino acid ester hydrochloride derivatives (commercially available) in anhydrous solvents. All reactions were carried out at room temperature under stirring conditions for 4 to 6 days in an inert atmosphere [42,97–106].

The activities of the pyrazole compound amino acids and the agar techniques determined **94–100**. The yeast of the F.o.a was isolated from a date palm touched by the vascular Fusarium prepared in a PDA medium at 37 g/L [54].

Based on Table 12, compared to blank culture, the inhibition rates of F.o.a development ranged from 0 to 480 mg/L for ester hydrochloride amino acids or their tripodal pyrazolic homologs. Inhibition activity against the growth of F.o.a. was shown by the various compounds studied, except **94** and **95**. However, the rate of this inhibition changes from one molecule to another. Compound **98** has the best antifungal activity due to methyl substituents as electron donor groups in methyl alaninate (alanine ester) as the amino acid; these products' structural and electronic diversity affected their biological activities. Further developments on this subject are currently in progress in order to understand their mechanistic interactions [54].

Table 12. MIC values of amino acids pyrazole compound tested against F.o.a.

ID	Structure	MIC (mg/L)
94		-
95		-
96		17
97		15
98		0.3
99		10
100		0.5

12. Comparison Using Structure–Activity Relationship

To understand this structure–activity relationship and the modes of action of these new biologically active molecules, we can carry out a theoretical study with bioinformatics molecular modeling (DFT, Docking, and ADME-Tox studies) after studying the mechanism of the reaction using conceptual DFT [107,108]. As a result, we obtained various prospective targeted drugs as inhibitors for Bayoud disease (Figure 2).

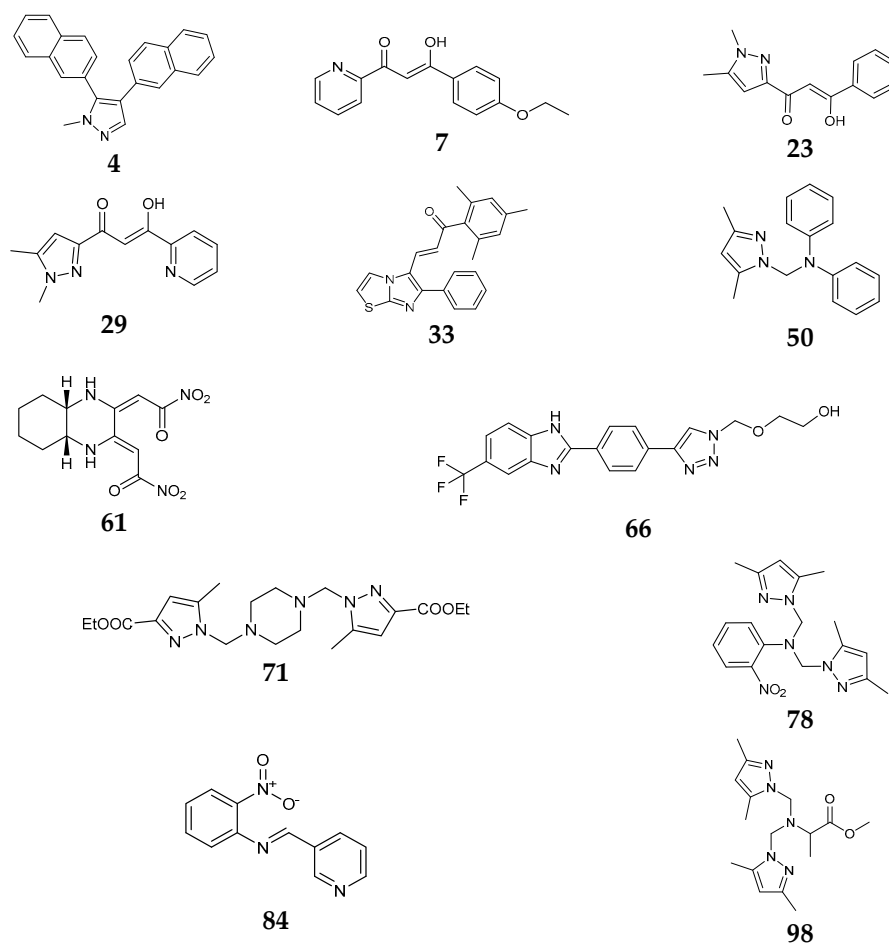


Figure 2. Chemical structure of the best active compounds from the group.

As presented in Figure 2, compounds 7, 23, 29, and 61 have the antifungal pharmacophore sites ($\delta^- \cdots \delta^-$) in common in N_1-O_4 , whereas other compounds have only one δ^- pharmacophore site pushed by the donor effect of the substituents on the phenyl rings; this specificity interferes in the biological activity against F.o.a.

13. Conclusions

This review uses 100 compounds of tested small molecules divided into ten classes against *Fusarium oxysporum* f. sp. *albedinis* (F.o.a). First, compound 4 ($IC_{50} = 99.1 \mu\text{g/mL}$) has the best fungus inhibition over all the pyrazole and imidazole derivatives, containing electron-donating character as para phenyl substituents. Furthermore, it displays high toxicity in the phenyl groups on the F.o.a. Second, from β keto-enol derivatives, compounds 7, 23, 29, and 61 have the antifungal pharmacophore sites ($\delta^- \cdots \delta^-$) in common in N_1-O_4 , whereas other compounds have only one δ^- pharmacophore site pushed by the donor effect of the substituents on the phenyl rings; this specificity interferes in the biological activity against F.o.a. Moreover, these products' structural and electronic diversity can affect their biological activities. Further developments on this subject are currently in progress to better understand their mechanistic interactions.

Funding: The review was funded by ANPMA/CNRST/UMP 2020–2023 Project, and Taif University Researchers Supporting Project TURSP2020/91, Taif, Saudi Arabia.

Acknowledgments: The authors thank the (ANPMA/CNRST/UMP 2020–2023 Project: Formulations fongiques, insecticide ou acaricides d’huiles essentielles des plantes aromatiques et médicinales et de leurs extraits aqueux) for their support. M.H.A expresses thanks to the Researchers Supporting Project TURSP2020/91 of Taif University, Taif, Saudi Arabia.

Conflicts of Interest: The authors declare no conflict of interest.

References

1. Ibrahim, E.B.; Mohamed, M.; Rafik, B. Bayoud disease of date palm in Algeria: History, epidemiology and integrated disease management. *Afr. J. Biotechnol.* **2015**, *14*, 542–550. [[CrossRef](#)]
2. Bouissil, S.; Guérin, C.; Roche, J.; Dubessay, P.; Alaoui-Talibi, E.; Pierre, G.; Michaud, P.; Mouzeyar, S.; Delattre, C.; El Modafar, C. Induction of Defense Gene Expression and the Resistance of Date Palm to *Fusarium oxysporum* f. sp. *Albedinis* in Response to Alginate Extracted from *Bifurcaria bifurcata*. *Mar. Drugs* **2022**, *20*, 88. [[PubMed](#)]
3. M’Hammed, E.; Fatiha, D.; Ayada, D.; Said, B.; Mohamed, K. Catalytic and synthesis of new compound based on geranium oil. *Egypt. J. Chem.* **2021**, *64*, 7341–7346. [[CrossRef](#)]
4. Belaidi, H.; Toumi-Benali, F.; Benzohra, I.E. Biocontrol of bayoud disease (*Fusarium oxysporum* f. sp. *albedinis*) on deglet-nour variety of date palm (*Phoenix dactylifera* L.) in south western oases of Algeria. *Agric. Sci. Digest* **2021**, *41*, 450–454. [[CrossRef](#)]
5. Komeil, D.A.; Abdalla, M.Y.; El-Bebany, A.F.; Basyony, A.B.A. Resistance marker detection in ten date palm cultivars to the wilt pathogen, *Fusarium oxysporum*. *Asian J. Plant Sci.* **2021**, *20*, 363–369. [[CrossRef](#)]
6. Tantaoui, A.; Ouinten, M.; Geiger, J.P.; Fernandez, D. Characterization of a single clonal lineage of *Fusarium oxysporum* f. sp. *albedinis* causing Bayoud disease of date palm in Morocco. *Phytopathology* **1996**, *86*, 787–792. [[CrossRef](#)]
7. Khalil, N.M.; Ali, H.M.; Ibrahim, A.E. Biochemical Activity of Propolis Alcoholic Extracts against *Fusarium oxysporum* hm89. *Egypt. J. Bot.* **2022**, *62*, 197–212. [[CrossRef](#)]
8. Shalaby, M.G.; Al-Hossainy, A.F.; Abo-Zeid, A.M.; Mobark, H.; Mahmoud, Y.A.G. Synthesis, characterization, physicochemical properties, and in-vitro anti-bacterial evaluation for doped Fe-Fusarium. *J. Mol. Str.* **2022**, *1259*, 132643. [[CrossRef](#)]
9. Hallasgo, A.M.; Hauser, C.; Steinkellner, S.; Hage-Ahmed, K. Single and coinoculation of Serendipita herbamans with arbuscular mycorrhizal fungi reduces Fusarium wilt in tomato and slows disease progression in the long-term. *Biol. Control* **2022**, *168*, 104876. [[CrossRef](#)]
10. Sedra, M.; Lazrek, B.H. *Fusarium oxysporum* f. sp. *Albedinis* Toxin Characterization and Use for Selection of Resistant Date Palm to Bayoud Disease; Springer: Cham, Switzerland, 2011; pp. 253–270.
11. Picot, S.; Beugnet, F.; Leboucher, G.; Bienvenu, A.-L. Drug resistant parasites and fungi from a one-health perspective: A global concern that needs transdisciplinary stewardship programs. *One Health* **2022**, *14*, 100368. [[CrossRef](#)]
12. Bankaitis, V.A.; Tripathi, A.; Chen, X.-R.; Igumenova, T.I. New strategies for combating fungal infections: Inhibiting inositol lipid signaling by targeting Sec14 phosphatidylinositol transfer proteins. *Adv. Biol. Reg.* **2022**, *84*, 100891. [[CrossRef](#)] [[PubMed](#)]
13. Alarjani, K.M.; Huessien, D.; Rasheed, R.A.; Kalaiyarasi, M. Green synthesis of silver nanoparticles by *Pisum sativum* L. (pea) pod against multidrug resistant foodborne pathogens. *J. King Saud Univ. Sci.* **2022**, *34*, 101897. [[CrossRef](#)]
14. Green, R.M.; Bicker, K.L. Development of an Anti-Biofilm Screening Technique Leads to the Discovery of a Peptoid with Efficacy against *Candida albicans*. *ACS Infect. Dis.* **2022**, *8*, 310–320. [[CrossRef](#)] [[PubMed](#)]
15. Vanzolini, T.; Bruschi, M.; Rinaldi, A.C.; Magnani, M.; Fraternali, A. Multitalented Synthetic Antimicrobial Peptides and Their Antibacterial, Antifungal and Antiviral Mechanisms. *Int. J. Mol. Sci.* **2022**, *23*, 545. [[CrossRef](#)] [[PubMed](#)]
16. Abrigach, F.; Rokni, Y.; Takfaoui, A.; Khoutoul, M.; Doucet, H.; Asehraou, A.; Touzani, R. In vitro screening, homology modeling and molecular docking studies of some pyrazole and imidazole derivatives. *Biomed. Pharmacother.* **2018**, *103*, 653–661. [[CrossRef](#)] [[PubMed](#)]
17. Madany, N.M.K.; Shehata, M.R.; Mohamed, A.S. Ovothiol—A isolated from sea urchin eggs suppress oxidative stress, inflammation, and dyslipidemia resulted in restoration of liver activity in cholestatic rats. *Biointerf. Res. Appl. Chem.* **2022**, *12*, 8152–8162.
18. Bulut, M.; Çelebi Sezer, Y.; Ceylan, M.M.; Alwazeer, D.; Koyuncu, M. Hydrogen-rich water can reduce the formation of biogenic amines in butter. *Food Chem.* **2022**, *384*, 132613. [[CrossRef](#)]
19. Dantas, T.S.; de Oliveira, A.M.; Ferreira, M.R.A.; Soares, L.A.L. Therapeutic potential of croton blanchetianus for the treatment of gastric ulcers: A brief review. *Biointerf. Res. Appl. Chem.* **2022**, *12*, 8219–8230.
20. Pakornchote, T.; Ektarawong, A.; Sukserm, A.; Pinsook, U.; Bovornratanaraks, T. Presence and absence of intrinsic magnetism in graphitic carbon nitrides designed through C–N–H building blocks. *Sci. Rep.* **2022**, *12*, 2343. [[CrossRef](#)]
21. Teng, Q.-H.; Sun, G.-X.; Luo, S.-Y.; Wang, K.; Liang, F.-P. Design, syntheses and antitumor activities evaluation of 1,5-diaryl substituted pyrazole secnidazole ester derivatives. *J. Heter. Chem.* **2021**, *58*, 1656–1664. [[CrossRef](#)]
22. Yang, Z.; Fang, Y.; Kim, J.-M.; Lee, K.-T.; Park, H. Synthesis of halogenated 1,5-diarylimidazoles and their inhibitory effects on lps-induced pge₂ production in raw 264.7 cells. *Molecules* **2021**, *26*, 6093. [[CrossRef](#)] [[PubMed](#)]
23. Mohamady, S.; Kralt, B.; Samwel, S.K.; Taylor, S.D. Efficient One-Pot, Two-Component Modular Synthesis of 3,5-Disubstituted Pyrazoles. *ACS Omega* **2018**, *3*, 15566–15574. [[CrossRef](#)] [[PubMed](#)]

24. Radi, S.; Tighadouini, S.; Feron, O.; Riant, O.; Bouakka, M.; Benabbes, R.; Mabkhot, Y.N. Synthesis of Novel beta-Keto-Enol Derivatives Tethered Pyrazole, Pyridine and Furan as New Potential Antifungal and Anti-Breast Cancer Agents. *Molecules* **2015**, *20*, 20186–20194. [[CrossRef](#)] [[PubMed](#)]
25. Tighadouini, S.; Benabbes, R.; Tillard, M.; Eddike, D.; Haboubi, K.; Karrouchi, K.; Radi, S. Synthesis, crystal structure, DFT studies and biological activity of (Z)-3-(3-bromophenyl)-1-(1,5-dimethyl-1H-pyrazol-3-yl)-3-hydroxyprop-2-en-1-one. *Chem. Cent. J.* **2018**, *12*, 122. [[CrossRef](#)] [[PubMed](#)]
26. Tighadouini, S.; Radi, S.; Abridgach, F.; Benabbes, R.; Eddike, D.; Tillard, M. Novel β -keto-enol Pyrazolic Compounds as Potent Antifungal Agents. Design, Synthesis, Crystal Structure, DFT, Homology Modeling, and Docking Studies. *J. Chem. Inf. Model.* **2019**, *59*, 1398–1409. [[CrossRef](#)]
27. Tighadouini, S.; Radi, S.; Benabbes, R.; Youssoufi, M.H.; Shityakov, S.; El Massaoudi, M.; Garcia, Y. Synthesis, Biochemical Characterization, and Theoretical Studies of Novel beta-Keto-enol Pyridine and Furan Derivatives as Potent Antifungal Agents. *ACS Omega* **2020**, *5*, 17743–17752. [[CrossRef](#)]
28. Koudad, M.; El Hamouti, C.; Elaatiaoui, A.; Dadou, S.; Oussaid, A.; Abridgach, F.; Pilet, G.; Benchat, N.; Allali, M. Synthesis, crystal structure, antimicrobial activity and docking studies of new imidazothiazole derivatives. *J. Iran. Chem. Soc.* **2019**, *17*, 297–306. [[CrossRef](#)]
29. Kassab, R.M.; Gomha, S.M.; Muhammad, Z.A.; El-Khouly, A.S. Synthesis, biological profile, and molecular docking of some new bis-imidazole fused templates and investigation of their cytotoxic potential as anti-tubercular and/or anticancer prototypes. *Med. Chem.* **2021**, *17*, 875–886. [[CrossRef](#)]
30. Haddad, Y.; Remes, M.; Adam, V.; Heger, Z. Toward structure-based drug design against the epidermal growth factor receptor (EGFR). *Drug Discov. Today* **2021**, *26*, 289–295. [[CrossRef](#)]
31. Abridgach, F.; Karzazi, Y.; Benabbes, R.; El Youbi, M.; Khoutoul, M.; Taibi, N.; Karzazi, N.; Benchat, N.; Bouakka, M.; Saalaoui, E.; et al. Synthesis, biological screening, P.O.M., and 3D-QSAR analyses of some novel pyrazolic compounds. *Med. Chem. Res.* **2017**, *26*, 1784–1795. [[CrossRef](#)]
32. Bandgar, B.P.; Gawande, S.S.; Bodade, R.G.; Gawande, N.M.; Khobragade, C.N. Synthesis and biological evaluation of a novel series of pyrazole chalcones as anti-inflammatory, antioxidant and antimicrobial agents. *Bioorg. Med. Chem.* **2009**, *17*, 8168–8173. [[CrossRef](#)] [[PubMed](#)]
33. Alegaon, S.G.; Alagawadi, K.R.; Garg, M.K.; Dushyant, K.; Vinod, D. 1,3,4-Trisubstituted pyrazole analogues as promising anti-inflammatory agents. *Bioorg. Chem.* **2014**, *54*, 51–59. [[CrossRef](#)] [[PubMed](#)]
34. Li, Y.R.; Li, C.; Liu, J.C.; Guo, M.; Zhang, T.Y.; Sun, L.P.; Zheng, C.J.; Piao, H.R. Synthesis and biological evaluation of 1,3-diaryl pyrazole derivatives as potential antibacterial and anti-inflammatory agents. *Bioorg. Med. Chem. Lett.* **2015**, *25*, 5052–5057. [[CrossRef](#)] [[PubMed](#)]
35. Khan, M.F.; Alam, M.M.; Verma, G.; Akhtar, W.; Akhter, M.; Shaquiquzzaman, M. The therapeutic voyage of pyrazole and its analogs: A review. *Eur. J. Med. Chem.* **2016**, *120*, 170–201. [[CrossRef](#)]
36. Alam, J.; Alam, O.; Alam, P.; Naim, M.J. A Review on Pyrazole chemical entity and Biological Activity. *Inter. J. Pharm. Sci. Res.* **2015**, *6*, 1433–1442.
37. Chovatia, P.T.; Akabari, J.D.; Kachhadia, P.K.; Zalavadia, P.D.; Joshi, H.S. Synthesis and selective antitubercular and antimicrobial inhibitory activity of 1-acetyl-3,5-diphenyl-4,5-dihydro-(1h)-pyrazole derivatives. *J. Serb. Chem. Soc.* **2006**, *71*, 713–720. [[CrossRef](#)]
38. Khanage, S.G.; Mohite, P.B.; Pandhare, R.B.; Raju, S.A. Microwave Assisted Synthesis of 1-[5-(Substituted Aryl)-1H-Pyrazol-3-yl]-3,5-Diphenyl-1H-1,2,4-Triazole as Antinociceptive and Antimicrobial Agents. *Adv. Pharm. Bull.* **2014**, *4*, 105–112.
39. Hamada, N.M.M.; Abdo, N.Y.M. Synthesis, characterization, antimicrobial screening and free-radical scavenging activity of some novel substituted pyrazoles. *Molecules* **2015**, *20*, 10468–10486. [[CrossRef](#)]
40. Elshaier, Y.A.; Barakat, A.; Al-Qahtany, B.M.; Al-Majid, A.M.; Al-Agamy, M.H. Synthesis of Pyrazole-Thiobarbituric Acid Derivatives: Antimicrobial Activity and Docking Studies. *Molecules* **2016**, *21*, 1337. [[CrossRef](#)]
41. Kucukguzel, S.G.; Coskun, I.; Aydin, S.; Aktay, G.; Gursoy, S.; Cevik, O.; Ozakpinar, O.B.; Ozsavci, D.; Sener, A.; Kaushik-Basu, N.; et al. Synthesis and characterization of celecoxib derivatives as possible anti-inflammatory, analgesic, antioxidant, anticancer and anti-HCV agents. *Molecules* **2013**, *18*, 3595–3614. [[CrossRef](#)]
42. El Kodadi, M.; Benamar, M.; Ibrahim, B.; Zyad, A.; Malek, F.; Touzani, R.; Ramdani, A.; Melhaoui, A. New synthesis of two tridentate bipyrazolic compounds and their cytotoxic activity tumor cell lines. *Nat. Prod. Res.* **2007**, *21*, 947–952. [[CrossRef](#)] [[PubMed](#)]
43. Insuasty, B.; Tigreros, A.; Orozco, F.; Quiroga, J.; Abonía, R.; Noguerras, M.; Sanchez, A.; Cobo, J. Synthesis of novel pyrazolic analogues of chalcones and their 3-aryl-4-(3-aryl-4,5-dihydro-1H-pyrazol-5-yl)-1-phenyl-1H-pyrazole derivatives as potential antitumor agents. *Bioorg. Med. Chem.* **2010**, *18*, 4965–4974. [[CrossRef](#)] [[PubMed](#)]
44. Yahyi, A.; Et-Touhami, A.; Yahyaoui, R.; Touzani, R. Synthesis, Characterization by Means of I.R., ¹H, ¹³C-N.M.R. and Biological Investigations on New Diorganotin Carboxylic Acid Derivatives. *Letts. Drug Des. Discov.* **2010**, *7*, 534–540. [[CrossRef](#)]
45. Ajay Kumar, K.; Jayaroopa, P. Pyrazoles: Synthetic strategies and their pharmaceutical applications-an overview. *Int. J. Pharm. Tech. Res.* **2013**, *5*, 1473–1486.
46. Kucukguzel, S.G.; Senkardes, S. Recent advances in bioactive pyrazoles. *Eur. J. Med. Chem.* **2015**, *97*, 786–815. [[CrossRef](#)]
47. Küçükgüzel, Ş.G.; Çikla-Süzgün, P. Recent advances bioactive 1,2,4-triazole-3-thiones. *Eur. J. Med. Chem.* **2015**, *97*, 830–870. [[CrossRef](#)]

48. Waring, M.J.; Ben-Hadda, T.; Kotchevar, A.T.; Ramdani, A.; Touzani, R.; El Kadiri, S.; Hakkou, A.; Bouakka, M.; Ellis, T. 2,3-Bifunctionalized quinoxalines: Synthesis, DNA interactions and evaluation of anticancer, anti-tuberculosis and antifungal activity. *Molecules* **2002**, *7*, 641–656. [[CrossRef](#)]
49. Ouahrouch, A.; Ighachane, H.; Taourirte, M.; Engels, J.W.; Sedra, M.H.; Lazrek, H.B. Benzimidazole-1,2,3-triazole hybrid molecules: Synthesis and evaluation for antibacterial/antifungal activity. *Arch. Pharm.* **2014**, *347*, 748–755. [[CrossRef](#)]
50. Radi, S.; Toubi, Y.; Hakkou, A.; Souna, F.; Himri, I.; Bouakka, M. Synthesis, Antibacterial and Antifungal Activities of Novel N,N'-bipyrazole Piperazine Derivatives. *Lett. Drug Des. Discov.* **2012**, *9*, 853–857. [[CrossRef](#)]
51. Klenc, J.; Raux, E.; Barnes, S.; Sullivan, S.; Duszynska, B.; Bojarski, A.J.; Strekowski, L. Synthesis of 4-Substituted 2-(4-Methylpiperazino) pyrimidines and Quinazoline Analogs as Serotonin 5-HT 2A Receptor Ligands. *J. Heter. Chem.* **2009**, *46*, 1259–1265.
52. Radi, S.; Toubi, Y.; Hamdani, I.; Hakkou, A.; Souna, F.; Himri, I.; Bouakka, M. Synthesis, antibacterial and antifungal activities of some new bipyrazolic tripodal derivatives. *Res. J. Chem. Sci.* **2012**, *2*, 40–44.
53. Toubi, Y.; Abrigach, F.; Radi, S.; Souna, F.; Hakkou, A.; Alsayari, A.; Muhsinah, A.B.; Mabkhot, Y.N. Synthesis, antimicrobial screening, homology modeling, and molecular docking studies of a new series of Schiff base derivatives as prospective fungal inhibitor candidates. *Molecules* **2019**, *24*, 3250. [[CrossRef](#)] [[PubMed](#)]
54. Boussalah, N.; Touzani, R.; Souna, F.; Himri, I.; Bouakka, M.; Hakkou, A.; Ghalem, S.; El Kadiri, S. Antifungal activities of amino acid ester functional pyrazolyl compounds against *Fusarium oxysporum* f. sp. *albedinis* and *Saccharomyces cerevisiae* yeast. *J. Saudi Chem. Soc.* **2013**, *17*, 17–21. [[CrossRef](#)]
55. Xing, A.; Zeng, D.; Chen, Z. Synthesis, crystal structure and antioxidant activity of butylphenol Schiff bases: Experimental and DFT study. *J. Mol. Str.* **2022**, *1253*, 132209. [[CrossRef](#)]
56. Aljamali, N.M.; Jawad, S.F. Preparation, spectral characterization, thermal study, and antifungal assay of (Formazane-mefenamic acid)-derivatives. *Egypt. J. Chem.* **2022**, *65*, 449–457. [[CrossRef](#)]
57. Jambulingam, M.; AnandaThangadurai, S.; Vijayabaskaran, M. Designing and Synthesis of Some Transition Metal Complexes Derived from Schiff Bases for Anti-Bacterial Activity. *J. Med. Chem. Sci.* **2022**, *5*, 10–18.
58. Mokhtari, P.; Mohammadnezhad, G. Anti-cancer properties and catalytic oxidation of sulfides based on vanadium (V) complexes of unprotected sugar-based Schiff-base ligands. *Polyhedron* **2022**, *215*, 115655. [[CrossRef](#)]
59. Murakami, M.; Kouyama, T. Crystal structure of squid rhodopsin. *Nature* **2008**, *453*, 363–367. [[CrossRef](#)]
60. Saavedra, C.P.; Encinas, M.V.; Araya, M.A.; Pichuanes, S.E.; Vásquez, C.C. Biochemical characterization of a thermostable cysteine synthase from *Geobacillus stearothermophilus* V. *Biochimie* **2004**, *86*, 481–485. [[CrossRef](#)]
61. Levitskiy, O.A.; Aglamazova, O.I.; Grishin, Y.K.; Nefedov, S.E.; Magdesieva, T.V. Corey-Chaykovsky cyclopropanation of dehydroalanine in the Ni(II) coordination environment: Electrochemical vs. chemical activation. *Electrochim. Acta* **2022**, *409*, 139980. [[CrossRef](#)]
62. Shenoy, K.V.; Venugopal, P.P.; Reena Kumari, P.D.; Chakraborty, D. Anti-corrosion investigation of a new nitro veratraldehyde substituted imidazopyridine derivative Schiff base on mild steel surface in hydrochloric acid medium: Experimental, computational, surface morphological analysis. *Mater. Chem. Phys.* **2022**, *281*, 125855. [[CrossRef](#)]
63. Hajri, A.K.; Jamoussi, B.; Albalawi, A.E.; Alhawiti, O.H.N.; Alsharif, A.A. Designing of modified ion-imprinted chitosan particles for selective removal of mercury (II) ions. *Carbohydr. Polym.* **2022**, *286*, 119207. [[CrossRef](#)] [[PubMed](#)]
64. Takfaoui, A.; Zhao, L.; Touzani, R.; Soulé, J.-F.; Dixneuf, P.H.; Doucet, H. One pot Pd(OAc)₂-catalysed 2,5-diarylation of imidazoles derivatives. *Tetrahedron* **2014**, *70*, 8316–8323. [[CrossRef](#)]
65. Takfaoui, A.; Zhao, L.; Touzani, R.; Dixneuf, P.H.; Doucet, H. Palladium-catalysed direct diarylations of pyrazoles with aryl bromides: A one step access to 4,5-diarylpyrazoles. *Tetrahedron Lett.* **2014**, *55*, 1697–1701. [[CrossRef](#)]
66. Wu, Z.B.; Park, H.Y.; Xie, D.W.; Yang, J.X.; Hou, S.T.; Shahzad, N.; Kim, C.K.; Yang, S. Synthesis, biological evaluation, and 3D-QSAR studies of N-(Substituted pyridine-4-yl)-1-(substituted phenyl)-5-trifluoromethyl-1H-pyrazole-4-carboxamide derivatives as potential succinate dehydrogenase inhibitors. *J. Agric. Food Chem.* **2021**, *69*, 1214–1223. [[CrossRef](#)]
67. Tighadouini, S.; Radi, S.; Garcia, Y. Selective chemical adsorption of Cd(II) on silica covalently decorated with a β -ketoenol-thiophene-furan receptor. *Mol. Syst. Des. Eng.* **2020**, *5*, 1037–1047. [[CrossRef](#)]
68. Radi, S.; Tighadouini, S.; Bacquet, M.; Degoutin, S.; Dacquin, J.-P.; Eddike, D.; Tillard, M.; Mabkhot, Y.N. β -Keto-enol Tethered Pyridine and Thiophene: Synthesis, Crystal Structure Determination and Its Organic Immobilization on Silica for Efficient Solid-Liquid Extraction of Heavy Metals. *Molecules* **2016**, *21*, 888. [[CrossRef](#)]
69. Radi, S.; Tighadouini, S.; Eddike, D.; Tillard, M.; Mabkhot, Y.N. Crystal Structure of (Z)-1-(1,5-dimethyl-1H-pyrazol-3-yl)-3-hydroxy-3-(4-methoxyphenyl)prop-2-en-1-one, C₁₅H₁₆N₂O₃. *Z. Kristallogr. New Cryst. Struct.* **2017**, *232*, 199–200. [[CrossRef](#)]
70. Radi, S.; Tighadouini, S.; Eddike, D.; Tillard, M.; Mabkhot, Y.N. Crystal Structure of (Z)-1-(1,5-dimethyl-1H-pyrazol-3-yl)-3-hydroxy-3-phenylprop-2-en-1-one, C₁₄H₁₄N₂O₂. *Z. Kristallogr. New Cryst. Struct.* **2017**, *232*, 201–202.
71. Radi, S.; Tighadouini, S.; Eddike, D.; Tillard, M.; Mabkhot, Y.N. Crystal Structure of (Z)-1-(1,5-dimethyl-1H-pyrazol-3-yl)-3-(4-ethoxyphenyl)-3-hydroxyprop-2-en-1-one, C₁₆H₁₈N₂O₃. *Z. Kristallogr. New Cryst. Struct.* **2017**, *232*, 207–208. [[CrossRef](#)]
72. Radi, S.; Tighadouini, S.; Eddike, D.; Tillard, M.; Mabkhot, Y.N. Crystal Structure of (Z)-1-(1,5-dimethyl-1H-pyrazol-3-yl)-3-hydroxy-3-(p-toly)prop-2-en-1-one, C₁₅H₁₆N₂O₂. *Z. Kristallogr. New Cryst. Struct.* **2017**, *232*, 209–210. [[CrossRef](#)]
73. Radi, S.; Tighadouini, S.; Eddike, D.; Tillard, M.; Mabkhot, Y.N. Crystal Structure of (Z)-3-hydroxy-3-(4-methoxyphenyl)-1-(pyridin-2-yl)prop-2-en-1-one, C₁₅H₁₃N₃O₃. *Z. Kristallogr. New Cryst. Struct.* **2017**, *232*, 235–236. [[CrossRef](#)]

74. Tighadouini, S.; Radi, S.; Ferbinteanu, M.; Garcia, Y. Highly Selective Removal of Pb(II) by a Pyridylpyrazole- β -ketoenol Receptor Covalently Bonded onto the Silica Surface. *ACS Omega* **2019**, *4*, 3954–3964. [[CrossRef](#)] [[PubMed](#)]
75. Peng, Y.-H.; Liao, F.-Y.; Tseng, C.-T.; Kuppusamy, R.; Li, A.S.; Chen, C.H.; Fan, Y.S.; Wang, S.Y.; Wu, M.H.; Hsueh, C.C.; et al. Unique Sulfur-Aromatic Interactions Contribute to the Binding of Potent Imidazothiazole Indoleamine 2,3-Dioxygenase Inhibitors. *J. Med. Chem.* **2020**, *63*, 1642–1659. [[CrossRef](#)]
76. Adole, V.A.; Jagdale, B.S.; Pawar, T.B.; Sagane, A.A. Ultrasound promoted stereoselective synthesis of 2,3-dihydrobenzofuran appended chalcones at ambient temperature. *S. Afr. J. Chem.* **2020**, *73*, 35–43. [[CrossRef](#)]
77. Morigi, R.; Vitali, B.; Prata, C.; Palomino, R.A.N.; Graziadio, A.; Locatelli, A.; Rambald, M.; Leoni, A. Investigation on the effects of antimicrobial imidazo[2,1-b]thiazole derivatives on the genitourinary microflora. *Med. Chem.* **2018**, *14*, 311–319. [[CrossRef](#)]
78. Abdel-Wahab, B.F.; Khidre, R.E.; Awad, G.E.A. Design and Synthesis of Novel 6-(5-Methyl-1H-1,2,3-triazol-4-yl)-5-[(2-(thiazol-2-yl)hydrazono)methyl]imidazo[2,1-b]thiazoles as Antimicrobial Agents. *J. Heter. Chem.* **2017**, *54*, 489–494. [[CrossRef](#)]
79. Jallapally, A.; Addla, D.; Yogeewari, P.; Sriram, D.; Kantevari, S. 2-Butyl-4-chloroimidazole based substituted piperazine-thiosemicarbazone hybrids as potent inhibitors of Mycobacterium tuberculosis. *Bioorg. Med. Chem. Lett.* **2014**, *24*, 5520–5524. [[CrossRef](#)]
80. Rani, N.; Sharma, A.; Gupta, G.K.; Singh, R. Imidazoles as potential antifungal agents: A review. *Med. Chem.* **2013**, *13*, 1626–1655. [[CrossRef](#)]
81. Mohamed, H.A.; Abdel-Wahab, B.F. Synthetic access to imidazo[2,1-b]thiazoles. *J. Sulf. Chem.* **2012**, *33*, 589–604. [[CrossRef](#)]
82. Abdel-Wahab, B.F.; Mohamed, H.A. Imidazobenzothiazoles: Synthesis and application. *J. Sulf. Chem.* **2012**, *33*, 335–349. [[CrossRef](#)]
83. Touzani, R.; Ramdani, A.; Ben-Hadda, T.; El Kadiri, S.; Maury, O.; Le Bozec, H.; Dixneuf, P.H. Efficient synthesis of new nitrogen donor containing tripods under microwave irradiation and without solvent. *Synth. Commun.* **2001**, *31*, 1315–1321. [[CrossRef](#)]
84. Lamsayah, M.; Khoutoul, M.; Abrigach, F.; Oussaid, A.; Touzani, R. Selective liquid-liquid extraction of Fe(II) and Cd(II) using n,n'-pyrazole bidentate ligands with theoretical study investigations. *Separ. Sci. Tech.* **2015**, *50*, 2170–2176.
85. Khoutoul, M.; Abrigach, F.; Zarrouk, A.; Benchat, N.-E.; Lamsayah, M.; Touzani, R. New nitrogen-donor pyrazole ligands for excellent liquid-liquid extraction of Fe²⁺ ions from aqueous solution, with theoretical study. *Res. Chem. Interm.* **2015**, *41*, 3319–3334. [[CrossRef](#)]
86. Touzani, R.; Ben-Hadda, T.; El Kadiri, S.; Ramdani, A.; Maury, O.; Le Bozec, H.; Toupet, L.; Dixneuf, P.H. Solution, solid state structure and fluorescence studies of 2,3-functiolized quinoxalines: Evidence for π -delocalized keto-enamine form with N-H...O intramolecular hydrogen bonds. *New J. Chem.* **2001**, *25*, 391–395. [[CrossRef](#)]
87. Daoud, A.; Cheknane, A.; Touzani, R.; Hilal, H.S.; Boulouiz, A. Simulation of the Electrochemical Properties of Dye-Sensitized Solar Cells Based on Quinoxaline Dyes: Effects of Hydroxyl Group Numbers and Positions. *J. Electr. Mater.* **2021**, *50*, 5656–5663. [[CrossRef](#)]
88. Bouabdallah, I.; Zidane, I.; Touzani, R.; Hacht, B.; Ramdani, A. Quinoxalines and tetraketones for metal cations extraction. *Arhivoc* **2006**, *10*, 77–81. [[CrossRef](#)]
89. Tornøe, C.W.; Christensen, C.; Meldal, M. Peptidotriazoles on Solid Phase: [1,2,3]-Triazoles by Regiospecific Copper(I)-Catalyzed 1,3-Dipolar Cycloadditions of Terminal Alkynes to Azides. *J. Org. Chem.* **2002**, *67*, 3057–3064. [[CrossRef](#)]
90. Rostovtsev, V.V.; Green, L.G.; Fokin, V.V.; Sharpless, K.B. A stepwise Huisgen cycloaddition process: Copper(I)-catalyzed regioselective “ligation” of azides and terminal alkynes. *Angew. Chem. Int. Ed.* **2002**, *41*, 2565–2599. [[CrossRef](#)]
91. Meldal, M.; Tornøe, C.W. Cu-Catalyzed Azide-Alkyne Cycloaddition. *Chem. Rev.* **2008**, *108*, 2952–3015. [[CrossRef](#)]
92. Pradere, U.; Roy, V.; Mc Brayer, T.R.; Schinazi, R.F.; Agrofoglio, L.A. Preparation of ribavirin analogues by copper- and ruthenium-catalyzed azide-alkyne 1,3-dipolar cycloaddition. *Tetrahedron* **2008**, *64*, 9044–9051. [[CrossRef](#)] [[PubMed](#)]
93. Al-Ghorbani, M.; Gouda, M.A.; Baashen, M.; Alharbi, O.; Almalki, F.A.; Ranganatha, L.V. Piperazine Heterocycles as Potential Anticancer Agents: A Review. *Pharm. Chem. J.* **2022**. [[CrossRef](#)]
94. Sanka, B.M.; Tadesse, D.M.; Bedada, E.T.; Mengesha, E.T.; Babu, G.N. Design, synthesis, biological screening and molecular docking studies of novel multifunctional 1,4-di (aryl/heteroaryl) substituted piperazine derivatives as potential antitubercular and antimicrobial agents. *Bioorg. Chem.* **2021**, *119*, 105568. [[CrossRef](#)] [[PubMed](#)]
95. Desai, N.C.; Rupala, Y.M.; Khasiya, A.G.; Shah, K.N.; Pandit, U.P.; Khedkar, V.M. Synthesis, biological evaluation, and molecular docking study of thiophene-, piperazine-, and thiazolidinone-based hybrids as potential antimicrobial agents. *J. Heter. Chem.* **2021**, *59*, 75–87. [[CrossRef](#)]
96. Harit, T.; Malek, F.; Ameduri, B. Fluorinated polymers based on pyrazole groups for fuel cell membranes. *Eur. Polym. J.* **2016**, *79*, 72–81. [[CrossRef](#)]
97. Garbacia, S.; Hillairet, C.; Touzani, R.; Lavastre, O. New nitrogen-rich tripodal molecules based on bis(pyrazol-1-ylmethyl)amines with substituents modulating steric hindrances and electron density of donor sites. *Collect. Czech. Chem. Commun.* **2005**, *70*, 34–40. [[CrossRef](#)]
98. Roh, S.-G.; Park, Y.-C.; Park, D.-K.; Kim, T.-J.; Jeong, J.H. Synthesis and characterization of a Zn(II) complex of a pyrazole-based ligand bearing a chiral L-alaninemethylester. *Polyhedron* **2001**, *20*, 1961–1965. [[CrossRef](#)]
99. Scarpellini, M.; Wu, A.J.; Kampk, J.W.; Pecoraro, V.L. Corroborative models of the cobalt(II) inhibited Fe/Mn superoxide dismutases. *Inorg. Chem.* **2005**, *44*, 5001–5010. [[CrossRef](#)]

100. Bouabdallah, I.; Touzani, R.; Zidane, I.; Ramdani, A. Synthesis of new tripodal ligand: N,N-bis[(1,5-dimethylpyrazol-3-yl)methyl]benzylamine. Catecholase activity of two series of tripodal ligands with some copper (II) salts. *Catal. Commun.* **2007**, *8*, 707–712. [[CrossRef](#)]
101. Touzani, R.; Garbacia, S.; Lavastre, O.; Yadav, V.K.; Carboni, B. Efficient solution phase combinatorial access to a library of pyrazole- and triazole-containing compounds. *J. Comb. Chem.* **2003**, *5*, 375–378. [[CrossRef](#)]
102. Touzani, R.; Vasapollo, G.; Scorrano, S.; Del Sole, R.; Manera, M.G.; Rella, R.; El Kadiri, S. New complexes based on tridentate bispyrazole ligand for optical gas sensing. *Mater. Chem. Phys.* **2011**, *126*, 375–380. [[CrossRef](#)]
103. Boussalah, N.; Touzani, R.; Bouabdallah, I.; El Kadiri, S.; Ghalem, S. Oxidation catalytic properties of new amino acid based on pyrazole tripodal ligands. *Int. J. Acad. Res.* **2009**, *1*, 137–143.
104. Boussalah, N.; Touzani, R.; Bouabdallah, I.; El Kadiri, S.; Ghalem, S. Synthesis, structure and catalytic properties of tripodal amino-acid derivatized pyrazole-based ligands. *J. Mol. Catal. A Chem.* **2009**, *306*, 113–117. [[CrossRef](#)]
105. Spadoni, G.; Balsamini, C.; Bedini, A.; Duranti, E.; Tontini, A. Short synthesis of tryptophane and β -carboline derivatives by reaction of indoles with N-(diphenylmethylene)- α,β -didehydroamino acid esters. *J. Heterocycl. Chem.* **1992**, *29*, 305–309. [[CrossRef](#)]
106. Zumbuehl, A.; Stano, P.; Sohrmann, M.; Dietiker, R.; Peter, M.; Carreira, E.M. Synthesis and investigation of tryptophan—Amphotericin B conjugates. *ChemBioChem* **2009**, *10*, 1617–1620. [[CrossRef](#)]
107. Qian, A.; Zheng, Y.; Wang, R.; Wei, J.; Cui, Y.; Cao, X.; Yang, Y. Design, synthesis, and structure-activity relationship studies of novel tetrazole antifungal agents with potent activity, broad antifungal spectrum and high selectivity. *Bioorg. Med. Chem. Lett.* **2017**, *28*, 344–350. [[CrossRef](#)]
108. Xiao, Z.P.; Ma, T.W.; Liao, M.L.; Feng, Y.T.; Peng, X.C.; Li, J.L.; Li, Z.P.; Wu, Y.; Luo, Q.; Deng, Y.; et al. Tyrosyl-tRNA synthetase inhibitors as antibacterial agents: Synthesis, molecular docking and structure-activity relationship analysis of 3-aryl-4-arylamino-furan-2(5H)-ones. *Eur. J. Med. Chem.* **2011**, *46*, 4904–4914. [[CrossRef](#)]